Microporous and Mesoporous Materials 158 (2012) 264–271

Contents lists available at SciVerse ScienceDirect

Microporous and Mesoporous Materials

journal homepage: www.elsevier.com/locate/micromeso

Theoretical insight into the minor role of paring mechanism in the methanol-to-olefins conversion within HSAPO-34 catalyst

Chuan-Ming Wang [a,*], Yang-Dong Wang [a], Hong-Xing Liu [a], Zai-Ku Xie [a,*], Zhi-Pan Liu [b]

[a] Shanghai Research Institute of Petrochemical Technology, SINOPEC, Shanghai 201208, China
[b] Department of Chemistry, Fudan University, Shanghai 200433, China

ARTICLE INFO

Article history:
Received 23 November 2011
Received in revised form 17 March 2012
Accepted 2 April 2012
Available online 9 April 2012

Keywords:
Methanol-to-olefins conversion
Density functional theory calculations
Reaction mechanism
HSAPO-34
Zeolites

ABSTRACT

Insight into the structure of hydrocarbon pool species and its effect on the catalytic activity and selectivity are urgently required in methanol-to-olefins (MTO) conversion. The fundamental issue is the understanding of its reaction mechanism. Previously, we have elucidated a complete catalytic cycle of side chain hydrocarbon pool mechanism. In this paper, paring hydrocarbon pool mechanism for different methylbenzenes (MBs) in HSAPO-34 zeotype catalyst is comprehensively investigated by periodic density functional theory calculations. The complete catalytic cycle involves a sequence of elementary steps that include methylation, ring contraction, shift of proton or methyl group, elimination of side alkyl groups, and regeneration of MBs. The major bottleneck is identified as the regeneration of MBs from five-membered ring cations. The intermediate cations having five-membered ring structure and the transition states featuring primary carbocations are unstable in the paring route. The overall energy barriers of different MBs depend strongly on the number of methyl groups. By comparing the kinetics of the paring route and the side chain route, we demonstrate that the full paring mechanism exhibits a higher barrier, and which is a minor route in the MTO conversion.

1. Introduction

The conversion of methanol to light olefins (methanol-to-olefins, MTO) catalyzed by zeolites (HZSM-5) or zeotype materials (HSAPO-34) has received much attention within chemical industry and academic community because it provides an attractive approach to produce ethene and propene from coal, oil, or biomass [1–18]. Besides ethene and propene, other alkenes, alkanes, aromatics are also produced in the MTO conversion. The complicated product distribution in the reaction makes the unveiling of the MTO reaction mechanism is a hot topic of ongoing debate [19–33].

Over the past two decades, more than 20 direct mechanisms were proposed to elucidate the formation of carbon–carbon bond from methanol. Now it is definitely verified that the direct coupling of C1 species cannot take place in the MTO reaction by lots of experimental and theoretical studies [34–36]. An indirect reaction mechanism, known as hydrocarbon pool mechanism, has therefore gained unanimous acceptance [37–43]. In this mechanism, certain organic reaction species known as the hydrocarbon pool serves as co-catalysts inside zeolites to which methanol is added and olefins are split off. Methylbenzenes (MBs) have been considered as the most active hydrocarbon pool species in a large number of studies [37,38]. Experimentally, Song et al. found that MBs with four to six methyl groups were more active and favored propene selectivity [44]. As for the evolution of MBs in the pore of catalysts, it was proposed that MBs may follow side chain route or paring route to eliminate light olefins from side alkyl chains in a closed catalytic cycle [21].

The side chain mechanism involves the deprotonation of methylbenzenium cations to form exocyclic double bond and the stepwise growth of the side alkyl chain by methylation of such exocyclic double bond. It has been extensively investigated by a large number of theoretical calculations [45–52]. The thermodynamics of the side chain hydrocarbon pool mechanism for MBs were calculated by Arstad et al. in gas phase and cluster model [45]. Their calculations placed the side chain route on a much stronger foundation and reproduced the experimental findings about the activity and selectivity of different MBs. Lesthaeghe et al. demonstrated the importance of the topology of zeolite framework on the gem-methylation of MBs as the first step in the side chain route using QM/MM method [46]. It was shown that CHA cages provide the perfect surroundings to stabilize methylbenzenium cations. More recently, we investigated a full catalytic cycle of side chain route for all MBs in HSAPO-34 using periodic model [49,50]. It was claimed that MBs with five and six methyl groups are not more active than those with fewer methyl groups, and propene is more favorable than ethene for all MBs. Similar conclusion about the selectivity was obtained by Lesthaeghe and

* Corresponding authors. Tel.: +86 21 68462197; fax: +86 21 68462283.
E-mail addresses: wangcm.sshy@sinopec.com (C.-M. Wang), xzk@sinopec.com (Z.-K. Xie).

1387-1811/$ - see front matter © 2012 Elsevier Inc. All rights reserved.
http://dx.doi.org/10.1016/j.micromeso.2012.04.004

co-workers when studying the side chain route in HZSM-5 model [47]. The elimination of side ethyl groups was identified as the major bottleneck in the MTO conversion.

The paring mechanism involves the ring contraction to form side alkyl chain and the ring expansion to regenerate the hydrocarbon pool. This route may be an alternative explanation for carbon label scrambling observed in experiments. Arstad et al. first theoretically investigated the evolution of heptamethylbenzenium (heptaMB$^+$) to form ethene, propene, and isobutene according to the paring route in the gas phase [53]. It is observed that the elimination of side alkyl group from alkylcyclopentadienyl cation is more difficult than from alkylbenzenium cation. Recently, this route was employed to link toluene to the largest cation observed in HZSM-5 zeolite using QM/MM method [54]. However, the paring route still needs to be thoroughly investigated not least because the direct comparison between the side chain route and the paring route is not possible when calculated using different computational models and methods.

Despite a long standing effort to elucidate and understand the hydrocarbon pool mechanism in the MTO reaction, some issues are still under debate. In particular, which route is dominant, and how the structures of hydrocarbon pool influence the catalytic activity and selectivity according to the proposed reaction mechanism. In this study, the paring route for different MBs inside HSAPO-34 zeotype catalyst is investigated extensively by periodic first-principles calculations in order to resolve the puzzles mentioned above. This paper is organized as follows. The calculation details and the modeling will be briefly summarized in Section 2. The detailed paring hydrocarbon pool route of MBs and its catalytic activity and selectivity are addressed in Section 3. The conclusions are drawn in Section 4.

2. Computational methods and modeling

All density functional theory (DFT) calculations with periodic boundary conditions (PBC) were performed using DMol^3 package as implemented in the Materials Studio software (version 4.3). The all electron double numerical basis set with polarization functions (DNP basis set) and the generalized gradient corrected Perdew–Burke–Ernzerhof (GGA-PBE) functional [55–58] were employed. The real space cutoff distance was 5.0 Å. The reciprocal-space integration over Brillouin zone was approximated by summing over a finite set of *k*-points with a grid separation of 0.05 Å^{-1} according to the Monkhorst–Pack scheme [59]. The eigenvector following method based on vibrational analysis was employed to search the transition state [60]. The convergence criteria for energy, force, and displacement were 2×10^{-5} hartree, 4×10^{-3} hartree/Å, and 5×10^{-3} Å, respectively. The DFT-D method was employed to correct the energy of a system by taking the dispersion effects into account [61,62].

The unit cell of HSAPO-34 zeotype catalyst is derived from CHA structure, in which all Si atoms were substituted by P and Al atoms alternatively, and then one P atom was replaced by Si atom [63]. In our simulation of reactions, all atoms in the cell are allowed to relax with the lattice constants being fixed. This model has been employed in a series of theoretical investigations on the MTO conversion [49–51,64]. Some calculated results are also checked using larger supercells.

3. Results and discussion

3.1. Paring mechanism for hexamethylbenzene (HMB) in HSAPO-34 catalyst

The paring hydrocarbon pool mechanism for HMB in zeolites is summarized in Scheme 1. The whole catalytic cycle begins with the gem-methylation of HMB to form heptaMB$^+$ (M2) cation. This is then followed by the ring contraction to form bicyclic intermediates (heptamethylbicyclo[3.1.0] hexenyl cation, M3). Starting from M3, the routes to yield propene and isobutene bifurcate. In the elimination of propene, an intramolecular H shift step leads to the formation of another bicyclic species (hexamethylbicyclo[3.2.0]heptenyl cation, M4/C3). Then one propene can be split off to leave pentamethylcyclopentadienyl cation (M5/C3). In the elimination of isobutene, an intramolecular methyl group shift results in the formation of cyclopentadienyl cation with a tert-butyl

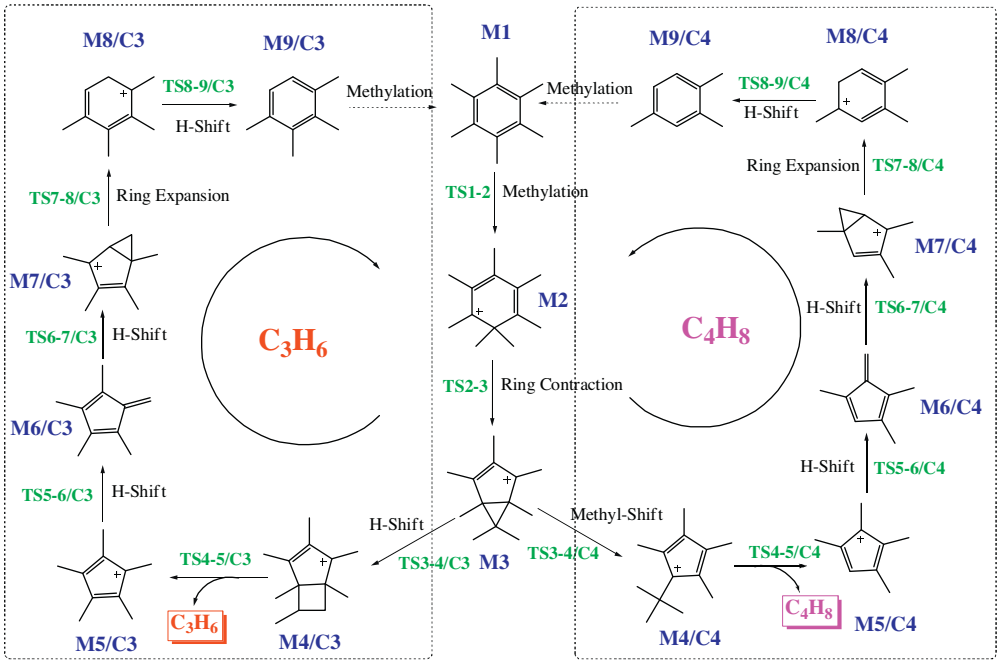

Scheme 1. Catalytic cycle of the paring hydrocarbon pool mechanism for the MTO conversion by HMB in acid zeolite or zeotype catalyst.

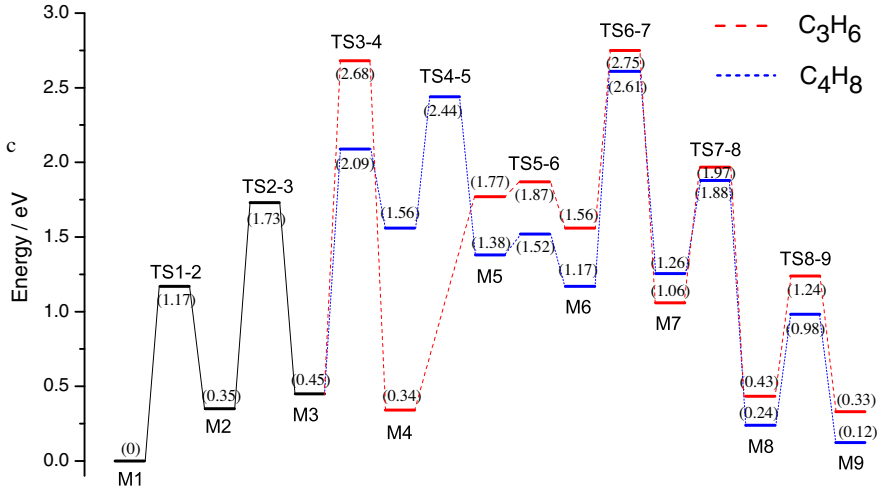

Fig. 1. Energy profile of the paring hydrocarbon pool mechanism for the MTO conversion in HMB/HSAPO-34. The relative energy of each state referred to M1 is listed in parenthesis.

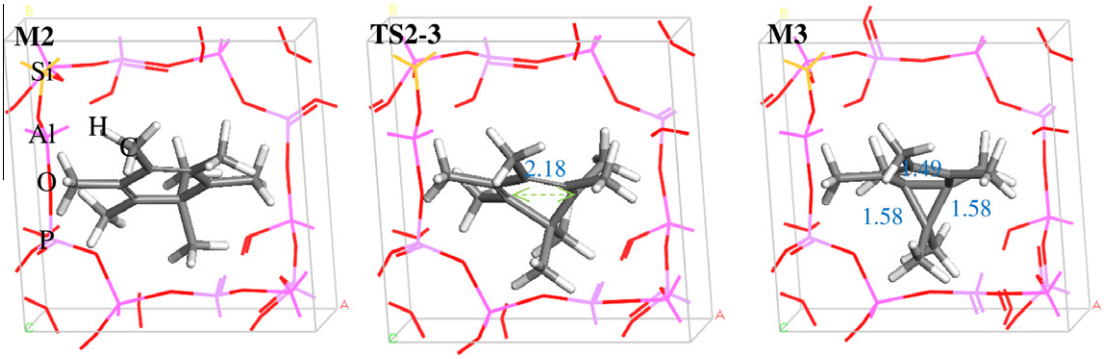

Fig. 2. Some involved structures in the formation of M3. The labeled distances are in Å.

group (M4/C4). The isobutene can be split off by intramolecular H shift with the tetramethylcyclopentadienyl cation (M5/C4) left. From M5 in both routes, the regeneration of HMB first involves the indirect intermolecular H shift to form the third bicyclic species (polymethylbicyclo[3.2.0]hexenyl cation, M7). M7 is then expanded to form polymethylbenzenium cation (M8). Finally, the abstraction of proton from M8 by zeolite framework and the subsequently repeated methylation regenerate HMB to close the catalytic cycle.

The calculated energy profile is shown in Fig. 1. Similar with the elucidation of the side chain hydrocarbon pool mechanism, the adsorption of one methanol in HMB/HSAPO-34 model is taken as the reference state (M1), and all the given energies are relative to that of M1. In the following, the calculated energies and the involved structures of intermediates and transition states (see Figs. 2–4) are addressed in detail.

The heptaMB$^+$ is formed through the methylation of the ring carbons of HMB by the adsorbed methanol, which needs to overcome an energy barrier of about 1.17 eV, and is endothermic by 0.35 eV. This step is same to that in side chain hydrocarbon pool mechanism [49]. The energy barrier of the subsequent ring contraction step (TS2–3) amounts to 1.38 eV, which is similar with that calculated in the gas phase (1.44 eV) [53]. The energy barrier with zero point energy (ZPE) correction for this step is 1.27 eV, just slightly smaller than that without ZPE correction. However, the stability of M3 varies by different models. In our model, M2 and M3 exhibit similar stability. But M3 is less stable than M2 by about 0.55 eV when calculated in the gas phase [53]. This indicates that zeolite framework can further stabilize bicyclic cation. In TS2–3, the C–C bond is shrunk from 2.53 to 2.18 Å. In M3, the formed C–C bond length is 1.49 Å (see Fig. 2).

In the elimination of propene process, one of proton in methyl group attached to the three-membered ring first shifts to the adjacent C atom. In TS3–4/C3, the breaking and forming C-H bond lengths are 1.58 and 1.19 Å, respectively (see Fig. 3). The three-membered carbon ring is broken, and the C-C distance is elongated from 1.58 to 2.45 Å. The energy barrier of this step is calculated to be 2.23 eV since the TS3–4/C3 state is primary carbocation. The energy of TS3–4/C3 referred to M2 is 2.33 eV, similar to that calculated in the gas phase (2.25 eV) [53]. It should be noted that the relative energy of M4/C3 is 0.34 eV, similar to those of M2 and M3. The simultaneously breaking of both C–C bonds in M4/C3 results in the elimination of propene and leaves pentamethylcyclopentadienyl cation. This process is endothermic by about 1.43 eV, and no transition state can be located. The energies of M5/C3 referred to M2 calculated by different models are similar (1.42 and 1.54 eV) [53].

The subsequent process involves the expansion of five-membered carbon ring to regenerate MB. The first step is the formation of bicyclic species. One of proton in substituted methyl group moves to the adjacent carbon ring and the side methylene attached one ring carbon. The direct intramolecular proton shift energy barrier of this step is 1.38 eV. However, another indirect intermolecular proton shift route is more plausible (0.98 eV). The proton is first

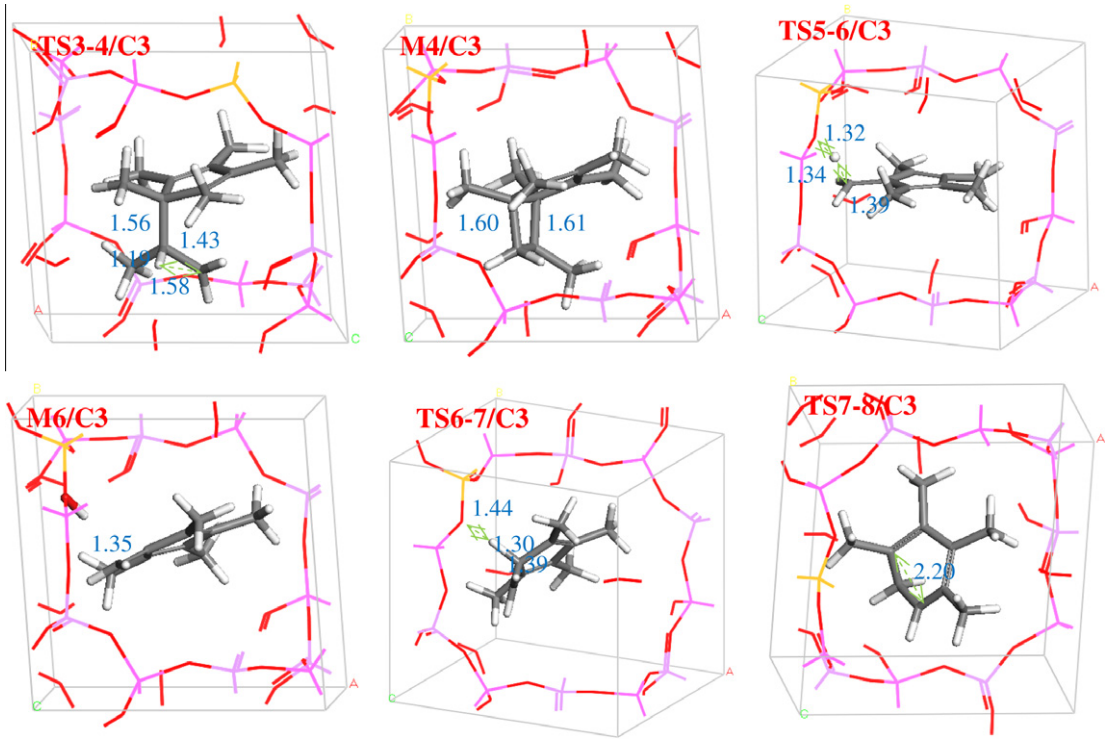

Fig. 3. Some involved structures in the elimination of propene and the regeneration of MB. The labeled distances are in Å.

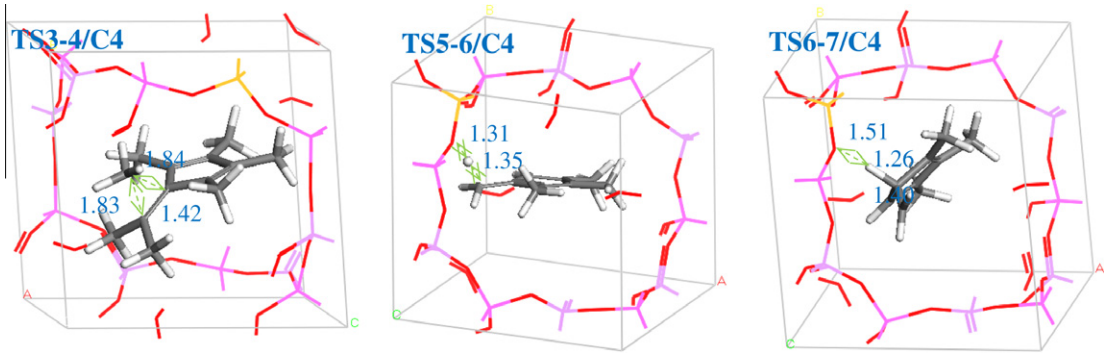

Fig. 4. Some involved structures in the elimination of isobutene and the regeneration of MB. The labeled distances are in Å.

abstracted by zeolite framework to form exocyclic double bond (M6/C3). Then this proton is donated to the carbon ring to form bicyclic species (M7/C3). In TS5–6/C3, the breaking C–H and forming O–H bond lengths are 1.34 and 1.32 Å, respectively (see Fig. 3). In TS6–7/C3, the forming C–H and breaking O–H bond lengths are 1.30 and 1.44 Å, respectively. The TS6–7/C3 state also features primary carbocation structure. The subsequent expansion of five-membered ring (TS7–8/C3) and deprotonation of polymethylbenzenium (TS8–9/C3) is relatively feasible.

In the other route to eliminate isobutene, one of methyl group is first shifted to the carbon atom in three-membered ring substituted by two methyl groups. The energy barrier of this step equals 1.64 eV, and is endothermic by 1.11 eV. In TS3–4/C4, the breaking and forming C–C bond lengths are 1.84 and 1.83 Å, respectively (see Fig. 4). The energy of TS3–4/C4 referred to M2 is 1.74 eV, same to that calculated in the gas-phase (1.73 eV). The formed M4/C4 in this route is very unstable compared to that in the elimination of propene route. The subsequent step (TS4–5/C4) is the elimination of side tert-butyl group to produce isobutene and tetramethylcyclopentadienyl cation. This step needs to overcome total energy of about 2.44 eV. The last process involves the regeneration of MB. The most difficult step in the regeneration is also the protonation of five-membered carbon ring with exocyclic double bond to form bicyclic species. The energy of TS6–7 in the production of isobutene is slightly lower than that in the production of propene.

As shown in Fig. 1, it can be found that the overall energy barriers of the formation of propene and isobutene by HMB in HSAPO-34 are respectively 2.75 and 2.61 eV in a closed catalytic cycle. The rate-determining step is the proton shift from zeolite framework to the ring carbon to form bicyclic species in the regeneration of MB (TS6–7). The intermediates M5 and M6 in both elimination routes and M4 in isobutene release route are very unstable since they are cyclopentadienyl cations. It was estimated that the radius (from terminal H atom to molecular center) of intermediate species within HSAPO-34 in M2, M3, and M4 states are in the range of 3.4–4.0 Å, and the occupied (Van der Waals) volume is around 200 $Å^3$.

Table 1
Energy barrier for the ring contraction step (TS2–3) by HMB within different HSAPO-34 supercells. All values are in eV.

Cell	Barrier	Cell	Barrier	Cell	Barrier
1 × 1 × 1	1.38				
1 × 1 × 2	1.43	1 × 2 × 1	1.28	2 × 1 × 1	1.36
1 × 2 × 2	1.35	2 × 1 × 2	1.45	2 × 2 × 1	1.36

In order to check whether the size of catalyst model affects the energy barrier, we calculated the energy barrier of ring contraction step (TS2–3) for HMB within different larger supercells of HSAPO-34 model. As can be seen from Table 1, the energy barrier of this step is in the range of 1.28–1.45 eV, and which is less sensitive to the size of used model. The computational model and method is thus reasonable to describe the system.

3.2. Paring mechanism for other MBs in HSAPO-34 catalyst

Besides HMB, other eight different MBs have also been considered in this study, including toluene, *p*-xylene (PX), *m*-xylene (MX), *o*-xylene (OX), 1,2,4-trimethylbenzene (TriMB), 1,2,3,5-tetramethylbenzene (TMB), 1,2,4,5-tetramethylbenzene, and pentamethylbenzene (PMB). According to the attack position of the carbon ring by methanol, twelve different pathways have been investigated for all MBs. They can be distinguished by the structure of benzenium cation M2 involved, as shown in Fig. 5. The labeling is same to our previous study of the side chain hydrocarbon pool mechanism for comparison [50]. The calculated energies of some important intermediates and transition states in different MB routes are listed in Table 2. In the following, the effect of additional methyl groups on the energy of some states referred to PX is addressed. It should be mentioned that it is essential to differentiate the position of additional methyl groups.

The stability of M2 intermediate can be enhanced with the number of additional methyl groups in the meta position. That is, PX > TriMB-A > TMB-A, TriMB-B > TMB-C > PMB-A, and TMB-B > PMB-B > HMB in relative state energy. This is because that the methyl groups in the meta position can help stabilize the benzenium cations via the resonance structures. On the other hand, the additional methyl groups in the ortho position can lower the magnitude of such effect.

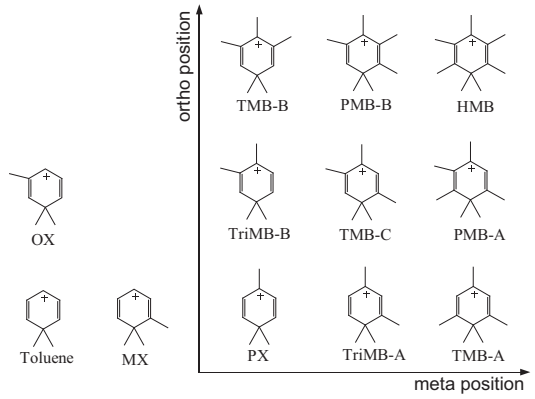

Fig. 5. The represented methylbenzenium cation M2 in each pathway.

As can be seen from Table 2, the ring contraction step (M2 → M3) is endothermic. In order to clearly address the effect of additional methyl groups, the energy barrier ($\Delta E^a(F)$) of this step is considered as the sum of the reverse reaction energy barrier ($\Delta E^a(B)$) and the reaction energy (ΔE_r). As shown in Table 3, a systematic decrease in ΔE and increase in $\Delta E^a(B)$ could be identified with the increase of the number of ortho methyl groups. In TMB-B, PMB-B, and HMB routes, M3 shows similar stability as M2. In other routes without ortho methyl group (PX, TriMB-A, TMB-A), M3 is less stable than M2 by about 0.83 to 0.98 eV. The presence of meta methyl groups has minor influence on the reaction energy. The magnitude of the effect of ortho methyl groups on ΔE_r is up to 0.80 eV. Nevertheless, the magnitude of the effect of ortho methyl groups on $\Delta E^a(B)$ can slightly be tuned by the meta methyl groups: the more the meta methyl groups, the less the effect of the ortho methyl groups. The magnitudes of $\Delta E^a(B)$ are 0.68, 0.57, and 0.49 eV corresponding to zero, one, and two meta methyl groups, respectively. To recap, it can be found that the ortho methyl groups can lower the barrier of the ring contraction step by about 0.10–0.39 eV. The forming C-C bond length of the TS2–3 in all pathways is in the range of 2.11 and 2.19 Å. The contraction barrier corrected by the DFT-D method to include the dispersion energy is also listed in Table 3. We found that the correction energy is at most 0.12 eV for this step, and the inclusion of dispersion interactions thus has minor influence on the calculated energy barrier.

The additional ortho methyl groups have a positive influence on the stability of intermediates and transition states having

Table 2
Energies of identified intermediates and transition states in the paring hydrocarbon pool mechanism for the MTO conversion catalyzed by different MBs in HSAPO-34 catalyst. Energies calculated using supercell (1 × 1 × 2) is listed in parentheses. All values are in eV.

MBs	Products	M2	TS2–3	M3	TS3–4	M4	TS4–5	M5	TS6–7	M9
HMB	C4	0.35 (0.32)	1.73	0.45	2.09	1.56	2.44	1.38	2.61 (2.77)	0.12
	C3				2.68	0.34		1.77	2.75 (2.97)	0.33
PMB-A	C4	0.47 (0.41)	1.89	0.95	2.13	1.60	2.49	1.65	2.79 (2.92)	0.07
	C3				2.75	0.70		2.14	2.98 (3.10)	0.49
PMB-B	C4	0.46 (0.48)	1.62	0.48	1.52	1.21	2.11	1.84	2.77 (3.03)	0.04
	C3				2.58	0.46		2.05	2.95 (3.16)	0.46
TMB-A	C4	0.32 (0.44)	2.09	1.30	2.70	2.46	2.94	2.56	3.62 (3.75)	0.56
	C4[54]	0.60	1.58	1.05	2.03	1.77	2.68			
	C3				3.11	1.27		2.50	3.49 (3.59)	1.03
TMB-B	C3	0.58 (0.72)	2.33	0.61	2.76	0.93		2.66	3.53 (3.66)	0.79
TMB-C	C4	0.60 (0.54)	1.92	1.02	1.43	1.15	2.93	2.64	3.05 (3.19)	0.12
	C3				2.73	0.84		2.40	3.05 (3.25)	0.59
TriMB-A	C4	0.49 (0.62)	1.91	1.34	2.09	2.51		3.13	3.58 (3.73)	0.71
	C3				2.99	1.09		2.74	3.78 (3.94)	0.73
TriMB-B	C3	0.73 (0.84)	2.52	1.03	3.02	1.20		3.10	3.73 (3.73)	0.80
PX	C3	0.72 (0.76)	2.58	1.54	2.92	1.28		3.68	4.09 (4.06)	1.22
OX	C3	0.91 (1.04)	2.66	1.25	3.17	1.59		3.52	3.93 (3.93)	1.06
MX	C4	0.72 (0.82)	2.30	1.61	2.50	2.46		3.85	3.97 (4.00)	1.10
	C3				3.32	1.14		3.56		
Toluene	C3	0.87	2.64	1.49	2.77	1.49		2.52		

Table 3
Energy barrier of the ring contraction step (TS2–3). Reaction energy and reverse energy barrier are shown in parentheses. The energy barrier corrected by DFT-D method is listed in square brackets. Number of additional methyl groups in the meta (column) and ortho (row) position is listed referred to PX. All values are in eV.

	0	1	2
2	1.76/[1.77] (0.04, 1.72)	1.16/[1.20] (0.02, 1.14)	1.38/[1.47] (0.10, 1.28)
1	1.79/[1.80] (0.31, 1.48)	1.32/[1.34] (0.42, 0.90)	1.42/[1.47] (0.49, 0.94)
0	1.86/[1.88] (0.83, 1.04)	1.41/[1.51] (0.84, 0.57)	1.77/[1.77] (0.98, 0.79)

five-membered ring structure, such as M3, M4, and TS3–4. These structures become more stable with additional ortho methyl groups. The magnitude of this effect on M3 intermediate is about 0.90 eV. For example, the energies of M3 in TMB-A, PMB-A, and HMB routes are 1.30, 0.95, and 0.45 eV, respectively. This can be attributed to the enhanced stability of bicyclic cation in the presence of additional ortho methyl groups via the resonance structures.

The magnitudes of the effect of the ortho methyl groups on TS3–4/C3 in the elimination of propene process are 0.26, 0.41, and 0.43 eV corresponding to zero, one, and two meta methyl groups, respectively. In addition, the influence on the stability of M4/C3 is more profound. The magnitudes are 0.35, 0.63, and 0.93 eV with the increase of the number of meta methyl groups. Similar trends are also observed in the elimination of isobutene process.

The stability of M5 is very sensitive of the number of substituted methyl groups on the five-membered ring. M5 become less stable with the decrease of the number of substituted methyl groups. It is found that the energy of M5 in HMB route is 1.77 eV where five methyl groups present on the ring, while the energy of which in PX route amounts to 3.68 eV where only one methyl group present in the elimination of propene process. The energy of M5 with four and one methyl groups in the elimination of isobutene process are 1.38 and 3.13 eV, respectively. Obviously, the enhanced stability of five-membered ring with more methyl groups is derived from resonance structures.

The energy of TS6–7 mainly correlates to the number of substituted methyl groups as well. In both elimination processes, TS6–7 becomes very unstable with the decrease of the number of methyl groups. The energy of TS6–7 is about 2.7–3.0 eV for HMB and PMB, which increases to 3.0–3.7 eV for TMB and TriMB, and finally it is as high as 4.0 eV for xylene. TS6–7 features primary carbocation structure. It is noted from Table 2 that the energy of TS6–7 is the overall energy barrier of the paring reaction route for all MB pathways. The regeneration of six-membered carbon ring is thus the rate-determining step in the paring route.

Recently, McCan et al. theoretically investigated the paring TMB-A route to link toluene to the pentamethylbenzenium cation in HZSM-5 model [54]. Some cited state energies in the elimination of isobutene are listed in Table 2. Despite of large energy difference in TS2–3, TS3–4 and M4, it can also be deduced that the step for the release of side tert–butyl group is energy demanding, and our calculated result in HSAPO-34 is comparable to that calculated in HZSM-5 (2.94 vs. 2.68 eV). The energy barrier of the ring expansion in M5 was 1.17 eV, slightly larger than our result (1.06 eV) as an indirect proton shift step is followed in our reaction route.

3.3. General discussions on the role of paring mechanism in the MTO conversion

We are now in the position to compare the catalytic activity and selectivity of different MBs following the paring route and the side chain route in HSAPO-34 model. The side chain pathway in HSAPO-34 has been extensively elaborated using identical methodology [49,50]. It was found that the overall energy barriers in the production of propene are in the range of 1.86 and 2.18 eV, and those in the production of ethene are in the range of 2.18 and 2.59 eV through side chain route [50]. However, the lowest overall energy barrier is 2.61 eV when through the paring route. As summarized in Fig. 6, the overall energy barriers of MBs to produce propene and isobutene through paring route are much larger than those to produce propene and ethene through side chain route, indicating that the paring mechanism may not be operative in the MTO conversion. This is in line with the previous experimental findings that the side chain methylation is the predominant pathway and the paring route is a possible minor pathway in HBeta zeolite [39].

In our previous work, we have demonstrated that MBs with five or six methyl groups are not more active than those with fewer methyl groups, and propene is intrinsically more favorable than ethene as the product through the side chain route [49,50]. By contrast, the overall energy barrier for MBs decreases with the number of substituted methyl groups when through the paring route, and isobutene is slightly preferential than propene as the product. The unstable states in the paring route include the intermediate cations having five-membered ring and the transition states featuring primary carbocations.

Experimentally, it was firstly concluded by Song et al. that the activity of MBs in HSAPO-34 increases with the average number of methyl groups per benzene ring [44]. In the experiment, methanol flow was abruptly ceased a predetermined time prior to quench. As no other methanol can be obtained after the quench, the decomposition of MBs may proceed through the paring route other than the side chain route. In the paring route, methanol only

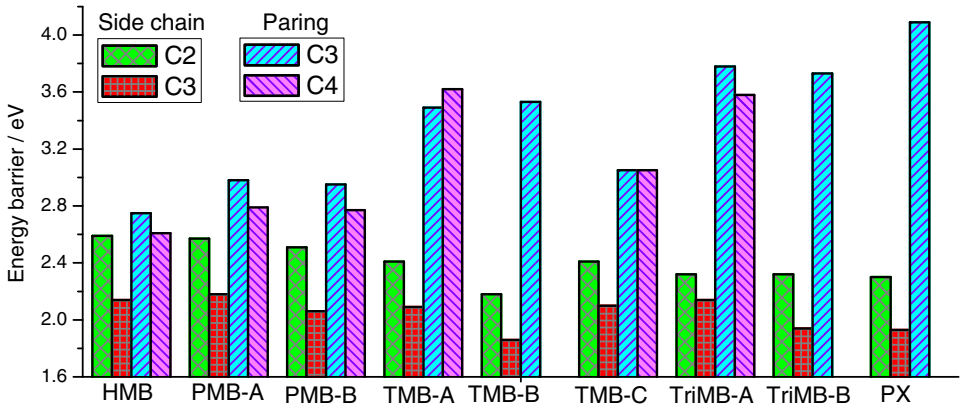

Fig. 6. Overall energy barriers of the MTO conversion catalyzed by different MBs in HSAPO-34 catalyst through the side chain route and the paring route. The energy barriers in the side chain route are cited from Ref. [50].

takes part in the steps to form benzenium cations and to regenerate MBs. Benzenium cations can readily be formed inside the cages prior to cessation. Very recently, hexamethylbenzenium cation has been directly observed using electron spin resonance (ESR) spectroscopy [65]. Olefins then may be split off through the paring route to leave cations with five-membered ring. Generally, the elimination energy barrier (from M1 to TS3–4 or TS4–5) increases with the decrease of the number of methyl groups in MBs, which may explain the experimental findings [44]. The cations with five-membered ring then may be decomposed into light olefins other than to regenerate MBs.

Despite of the results that the side chain route may be the predominant pathway within hydrocarbon pool mechanism, the inconsistency between experimental findings and theoretical results is still exist. One debate is the effect of MB structure on catalytic activity and selectivity. Furthermore, the overall energy barriers in the side chain route is calculated to be high as well [50]. As we addressed previously, the study only focused on MBs as the hydrocarbon pool may result in a biased understanding on the MTO conversion [50]. The pursuit of other hydrocarbon pool species is therefore required. Recently, Svelle et al. introduced a dual cycle mechanism in which propene and higher alkenes are preferentially produced by the alkene methylation and interconversions [41–43]. This was then confirmed by recent theoretical calculations [66].

According to our preliminary calculation results, we believe that alkene methylation and cracking mechanism, firstly proposed by Dessau, should deserve more attention in the MTO conversion [67]. The overall energy barriers for the production of ethene and propene are much lower than those in side chain and paring hydrocarbon pool mechanism. That is to say, hydrocarbon pool mechanism where alkenes themselves are the organic active centers may be operative in the MTO conversion. The detailed work on this topic is now under progress.

4. Conclusion

In summary, the detailed paring hydrocarbon pool mechanism of nine different MBs (from toluene to HMB) in the pore of HSAPO-34 zeotype catalyst for the MTO conversion has been investigated systematically from first-principles. This work at the atomic level can help to establish a complete picture about the paring route and to provide a fundamental insight into the role of MBs. It is demonstrated that the side chain route rather than the paring route is the predominant pathway within the hydrocarbon pool mechanism where MBs are organic active species. This is consistent with the experimental results on HBeta zeolite. The overall barrier of MBs through the paring route decreases with the number of methyl groups per benzene ring. The rate-determining step of the reaction is the proton shift from inorganic framework to the ring carbon to form bicyclic species in the regeneration of six-membered carbon ring. In the paring route, only propene and isobutene is considered as the products. Therefore, we can conclude that light olefins such as ethene and propene in the MTO reaction cannot be produced through the paring hydrocarbon pool mechanism.

Acknowledgements

This work is supported by National Basic Research Program of China (2009CB623504), National Science Foundation of China (21103231), and Shanghai Science Foundation (11ZR1449700).

References

[1] Y. Traa, Chem. Commun. 46 (2010) 2175–2187.
[2] M. Stocker, Micropor. Mesopor. Mater. 29 (1999) 3–48.
[3] S. Lopez-Orozco, A. Inayat, A. Schwab, T. Selvam, W. Schwieger, Adv. Mater. 23 (2011) 2602–2615.
[4] J. Freiding, B. Kraushaar-Czarnetzki, Appl. Catal. A: Gen. 391 (2011) 254–260.
[5] D.S. Wragg, D. Akporiaye, H. Fjellvag, J. Catal. 279 (2011) 397–402.
[6] L. Sommer, A. Krivokapic, S. Svelle, K.P. Lillerud, M. Stocker, U. Olsbye, J. Phys. Chem. C 115 (2011) 6521–6530.
[7] J. Li, Y. Wei, G. Liu, Y. Qi, P. Tian, B. Li, Y. He, Z. Liu, Catal. Today 171 (2011) 221–228.
[8] Y. Kumita, J. Gascon, E. Stavitski, J.A. Moulijn, F. Kapteijn, Appl. Catal. A: Gen. 391 (2011) 234–243.
[9] W. Dai, X. Wang, G. Wu, N. Guan, M. Hunger, L. Li, ACS Catal. 1 (2011) 292–299.
[10] F. Bleken, W. Skistad, K. Barbera, M. Kustova, S. Bordiga, P. Beato, K.P. Lillerud, S. Svelle, U. Olsbye, Phys. Chem. Chem. Phys. 13 (2011) 2539–2549.
[11] K. Barbera, F. Bonino, S. Bordiga, T.V.W. Janssens, P. Beato, J. Catal. 280 (2011) 196–205.
[12] H.-K. Min, M.B. Park, S.B. Hong, J. Catal. 271 (2010) 186–194.
[13] J.H. Lee, M.B. Park, J.K. Lee, H.-K. Min, M.K. Song, S.B. Hong, J. Am. Chem. Soc. 132 (2010) 12971–12982.
[14] S. Teketel, S. Svelle, K.-P. Lillerud, U. Olsbye, ChemCatChem 1 (2009) 78–81.
[15] S. Ivanova, C. Lebrun, E. Vanhaecke, C. Pham-Huu, B. Louis, J. Catal. 265 (2009) 1–7.
[16] M. Castro, S.J. Warrender, P.A. Wright, D.C. Apperley, Y. Belmabkhout, G. Pirngruber, H.-K. Min, M.B. Park, S.B. Hong, J. Phys. Chem. C 113 (2009) 15731–15741.
[17] F. Bleken, M. Bjorgen, L. Palumbo, S. Bordiga, S. Svelle, K.P. Lillerud, U. Olsbye, Top. Catal. 52 (2009) 218–228.
[18] Q. Zhu, J.N. Kondo, T. Tatsumi, S. Inagaki, R. Ohnuma, Y. Kubota, Y. Shimodaira, H. Kobayashi, K. Domen, J. Phys. Chem. C 111 (2007) 5409–5415.
[19] J.F. Haw, W.G. Song, D.M. Marcus, J.B. Nicholas, Acc. Chem. Res. 36 (2003) 317–326.
[20] J.F. Haw, D.M. Marcus, Top. Catal. 34 (2005) 41–48.
[21] U. Olsbye, M. Bjorgen, S. Svelle, K.P. Lillerud, S. Kolboe, Catal. Today 106 (2005) 108–111.
[22] Z.M. Cui, Q. Liu, W.G. Song, L.J. Wan, Angew. Chem., Int. Ed. 45 (2006) 6512–6515.
[23] P. Sazama, B. Wichterlova, J. Dedecek, Z. Tvaruzkova, Z. Musilova, L. Palumbo, S. Sklenak, O. Gonsiorova, Micropor. Mesopor. Mater. 143 (2011) 87–96.
[24] D. Mores, J. Kornatowski, U. Olsbye, B.M. Weckhuysen, Chem. Eur. J. 17 (2011) 2874–2884.
[25] W. Dai, M. Scheibe, N. Guan, L. Li, M. Hunger, ChemCatChem 3 (2011) 1130–1133.
[26] M. Vandichel, D. Lesthaeghe, J. Van der Mynsbrugge, M. Waroquier, V. Van Speybroeck, J. Catal. 271 (2010) 67–78.
[27] W. Dai, W. Kong, L. Li, G. Wu, N. Guan, N. Li, ChemCatChem 2 (2010) 1548–1551.
[28] M. Bjorgen, S. Akyalcin, U. Olsbye, S. Benard, S. Kolboe, S. Svelle, J. Catal. 275 (2010) 170–180.
[29] D.S. Wragg, R.E. Johnsen, M. Balasundaram, P. Norby, H. Fjellvag, A. Gronvold, T. Fuglerud, J. Hafizovic, O.B. Vistad, D. Akporiaye, J. Catal. 268 (2009) 290–296.
[30] B.P.C. Hereijgers, F. Bleken, M.H. Nilsen, S. Svelle, K.P. Lillerud, M. Bjorgen, B.M. Weckhuysen, U. Olsbye, J. Catal. 264 (2009) 77–87.
[31] D. Mores, E. Stavitski, M.H.F. Kox, J. Kornatowski, U. Olsbye, B.M. Weckhuysen, Chem. Eur. J. 14 (2008) 11320–11327.
[32] L. Palumbo, F. Bonino, P. Beato, M. Bjorgen, A. Zecchina, S. Bordiga, J. Phys. Chem. C 112 (2008) 9710–9716.
[33] W.G. Song, D.M. Marcus, H. Fu, J.O. Ehresmann, J.F. Haw, J. Am. Chem. Soc. 124 (2002) 3844–3845.
[34] D. Lesthaeghe, V. Van Speybroeck, G.B. Marin, M. Waroquier, Angew. Chem., Int. Ed. 45 (2006) 1714–1719.
[35] D.M. Marcus, K.A. McLachlan, M.A. Wildman, J.O. Ehresmann, P.W. Kletnieks, J.F. Haw, Angew. Chem., Int. Ed. 45 (2006) 3133–3136.
[36] Y.D. Wang, C.M. Wang, H.X. Liu, Z.K. Xie, Chin. J. Catal. 31 (2010) 33–37.
[37] B. Arstad, S. Kolboe, J. Am. Chem. Soc. 123 (2001) 8137–8138.
[38] W.G. Song, J.F. Haw, J.B. Nicholas, C.S. Heneghan, J. Am. Chem. Soc. 122 (2000) 10726–10727.
[39] A. Sassi, M.A. Wildman, H.J. Ahn, P. Prasad, J.B. Nicholas, J.F. Haw, J. Phys. Chem. B 106 (2002) 2294–2303.
[40] M. Bjorgen, U. Olsbye, D. Petersen, S. Kolboe, J. Catal. 221 (2004) 1–10.
[41] S. Svelle, U. Olsbye, F. Joensen, M. Bjorgen, J. Phys. Chem. C 111 (2007) 17981–17984.
[42] M. Bjorgen, S. Svelle, F. Joensen, J. Nerlov, S. Kolboe, F. Bonino, L. Palumbo, S. Bordiga, U. Olsbye, J. Catal. 249 (2007) 195–207.
[43] S. Svelle, F. Joensen, J. Nerlov, U. Olsbye, K.P. Lillerud, S. Kolboe, M. Bjorgen, J. Am. Chem. Soc. 128 (2006) 14770–14771.
[44] W.G. Song, H. Fu, J.F. Haw, J. Am. Chem. Soc. 123 (2001) 4749–4754.
[45] B. Arstad, J.B. Nicholas, J.F. Haw, J. Am. Chem. Soc. 126 (2004) 2991–3001.
[46] D. Lesthaeghe, B. De Sterck, V. Van Speybroeck, G.B. Marin, M. Waroquier, Angew. Chem., Int. Ed. 46 (2007) 1311–1314.
[47] D. Lesthaeghe, A. Horre, M. Waroquier, G.B. Marin, V. Van Speybroeck, Chem. Eur. J. 15 (2009) 10803–10808.
[48] D. Lesthaeghe, V. Van Speybroeck, M. Waroquier, Phys. Chem. Chem. Phys. 11 (2009) 5222–5226.
[49] C.M. Wang, Y.D. Wang, Z.K. Xie, Z.P. Liu, J. Phys. Chem. C 113 (2009) 4584–4591.
[50] C.M. Wang, Y.D. Wang, H.X. Liu, Z.K. Xie, Z.P. Liu, J. Catal. 271 (2010) 386–391.

[51] C.M. Wang, Y.D. Wang, H.X. Liu, Z.K. Xie, Z.P. Liu, Acta Chim. Sinica 68 (2010) 2312–2318.
[52] K. Hemelsoet, A. Nollet, V. Van Speybroeck, M. Waroquier, Chem. Eur. J. 17 (2011) 9083–9093.
[53] B. Arstad, S. Kolboe, O. Swang, J. Phys. Chem. A 109 (2005) 8914–8922.
[54] D.M. McCann, D. Lesthaeghe, P.W. Kletnieks, D.R. Guenther, M.J. Hayman, V. Van Speybroeck, M. Waroquier, J.F. Haw, Angew. Chem., Int. Ed. 47 (2008) 5179–5182.
[55] B. Delley, J. Chem. Phys. 113 (2000) 7756–7764.
[56] B. Delley, Phys. Rev. B 66 (2002) 155125.
[57] J.P. Perdew, K. Burke, M. Ernzerhof, Phys. Rev. Lett. 77 (1996) 3865–3868.
[58] B. Delley, J. Chem. Phys. 92 (1990) 508–517.
[59] H.J. Monkhorst, J.D. Pack, Phys. Rev. B 13 (1976) 5188–5192.
[60] A. Banerjee, N. Adams, J. Simons, R. Shepard, J. Phys. Chem. 89 (1985) 52–57.
[61] S. Grimme, J. Comput. Chem. 27 (2006) 1787–1799.
[62] S. Grimme, J. Comput. Chem. 25 (2004) 1463–1473.
[63] B.M. Lok, C.A. Messina, R.L. Patton, R.T. Gajek, T.R. Cannan, E.M. Flanigen, J. Am. Chem. Soc. 106 (1984) 6092–6093.
[64] F. Bleken, S. Svelle, K.P. Lillerud, U. Olsbye, B. Arstad, O. Swang, J. Phys. Chem. A 114 (2010) 7391–7397.
[65] S.J. Kim, H.-G. Jang, J.K. Lee, H.-K. Min, S.B. Hong, G. Seo, Chem. Commun. 47 (2011) 9498–9500.
[66] D. Lesthaeghe, J. Van der Mynsbrugge, M. Vandichel, M. Waroquier, V. Van Speybroeck, ChemCatChem 3 (2011) 208–212.
[67] R.M. Dessau, J. Catal. 99 (1986) 111–116.